# COMPUTED ELECTRON MICROSCOPE IMAGES OF LINES OF DILATION

## By P. Humble*

### Summary

Theoretical micrographs of the electron microscope images of lines of dilation in elastically isotropic crystals have been computed. The symmetry properties, the condition for invisibility, and the intensity of the images compared with those of dislocations have been investigated.

## Introduction

This paper describes the properties of the bright-field electron microscope images of lines of dilation contained in thin foils of elastically isotropic materials. Some of the properties of these defects have been discussed previously by Blank and Amelinckx (1963), and Ashby and Brown (1963) have made a similar study of centres of dilation. In the present paper, computed electron micrographs (Head 1967; Humble 1968a) are shown which illustrate the symmetry properties, the condition for invisibility, and the intensity of images of lines of expansion and contraction compared with those of a dislocation. Since the detection and identification of a particular defect is often aided by a knowledge of the images to be expected, the micrographs presented here may be of assistance in the experimental identification of lines of dilation.

## Theoretical

The calculations are based on isotropic elasticity and the displacements around the defect are derived from those around a hollow circular cylinder under internal pressure in an infinite solid given by Coker and Filon (1957). The displacements are radial and their magnitude $u$ at a distance $r$ from the line of dilation may be written as

$$u = \epsilon \Delta\epsilon / r, \tag{1}$$

where $\epsilon$ is the radius of the cylinder and $\Delta\epsilon$ is the value of the displacement at $r = \epsilon$. Negative values of $\Delta\epsilon$ signify a contraction about the line rather than an expansion.

Displacements of this form have been incorporated into a programme of the type described by Head (1967) and Humble (1968a) to calculate the bright-field electron diffraction images of the defect under two-beam conditions. The micrographs are computed using the column approximation of Howie and Whelan (1961, 1962) including absorption. The thickness of the foils has been taken as approximately 1800 Å, and the reflecting vectors used are appropriate for a face-centred cubic material. The values of extinction distances for nickel have been used (Hirsch *et al.* 1965). Unless otherwise stated, the contrast of the grey scale that has been used to produce the micrographs is such that the symbol representing background intensity (a dot) changes to its neighbouring symbols at 15% above and 7% below background intensity.

* Division of Tribophysics, CSIRO, University of Melbourne, Parkville, Vic. 3052.

Results

Figure 1 shows the micrographs of a line of expansion taken under the eight low order reflections contained in the [001] beam direction. The foil normal is [$\bar{1}15$] and the direction of the line is [314]. This crystallography has been chosen as being representative of a general case, imposing no special symmetry conditions. The dimensionless deviation from the Bragg condition, $w$, is 0·6. The value of $\Delta\epsilon$ at a radius $\epsilon$ of 3 atomic distances has been taken as $\epsilon$. These conditions are equivalent to considering a row of large impurity atoms.

The first thing of note is that the images all exhibit periodic variations in width and intensity along their length appropriate to the effective extinction distance for the particular reflecting vector. This is similar to the behaviour of dislocation images. However, the images of the dilation have a symmetry which is different to that found in dislocation images. Images of lines of dilation always contain a centre of inversion, whereas in general this is not true for dislocation images.* The inversion symmetry of lines of dilation is clearly illustrated in the micrographs in Figure 1.

Changing the reflecting vector, $g$, from $+g$ to $-g$ results in the inversion of the bright-field image of a dislocation about the centre of the image, i.e. the image is reversed with respect to the top and bottom surfaces of the foil and side for side with respect to the dislocation line. It may be seen from the micrographs in Figure 1 that no such inversion occurs for the images of line dilations. Indeed, it may be deduced from the form of the displacements that, in general, the image of a line of dilation taken under a reflecting vector $g$ bears no relation to that obtained using a reflecting vector $-g$; again, this effect is clearly shown in Figure 1. The one exception to this is when the line of dilation, the beam direction, and the reflecting vector are mutually perpendicular. This case is illustrated in Figures 2(a) and 2(b) and it may be seen that the images are related by a reflection operation about the line of the dilation. In these micrographs the direction of the line of dilation is [$0\bar{1}1$], the beam direction is [011], and the reflecting vectors are 200 and $\bar{2}00$ respectively. The foil normal is [001].

Another effect concerning the symmetry of the image occurs in cases when the line of dilation is imaged in turn with two reflecting vectors of the same type which are inclined at the same angle to the line. Under these conditions, the two micrographs of the line of dilation are identical. This effect is illustrated for the $31\bar{1}$ and $3\bar{1}1$ reflecting vectors in Figures 2(c) and 2(d); the other parameters used in computing these micrographs are the same as for Figures 2(a) and 2(b). Because of the general "skewing" effect on an image due to the non-coincidence of the foil normal and beam direction (Head, Loretto, and Humble 1967; Humble 1968a), this effect is limited to cases such as those shown in Figure 2, where the foil normal, the line

---

* If a dislocation image did have a centre of inversion, the dislocation with opposite Burgers vector would have the same image (Howie and Whelan 1962). However, Head (1969) has shown that, in general, different dislocations must have different images except possibly for some specific combinations of $w$, foil thickness, and anomalous absorption. Although it has not yet been shown for all these combinations, it is known that for the particular case of zero $w$, zero anomalous absorption, and any foil thickness all dislocation images have a centre of inversion. However, in general, the critical combinations of these three parameters lie far away from those used in normal electron microscopy.
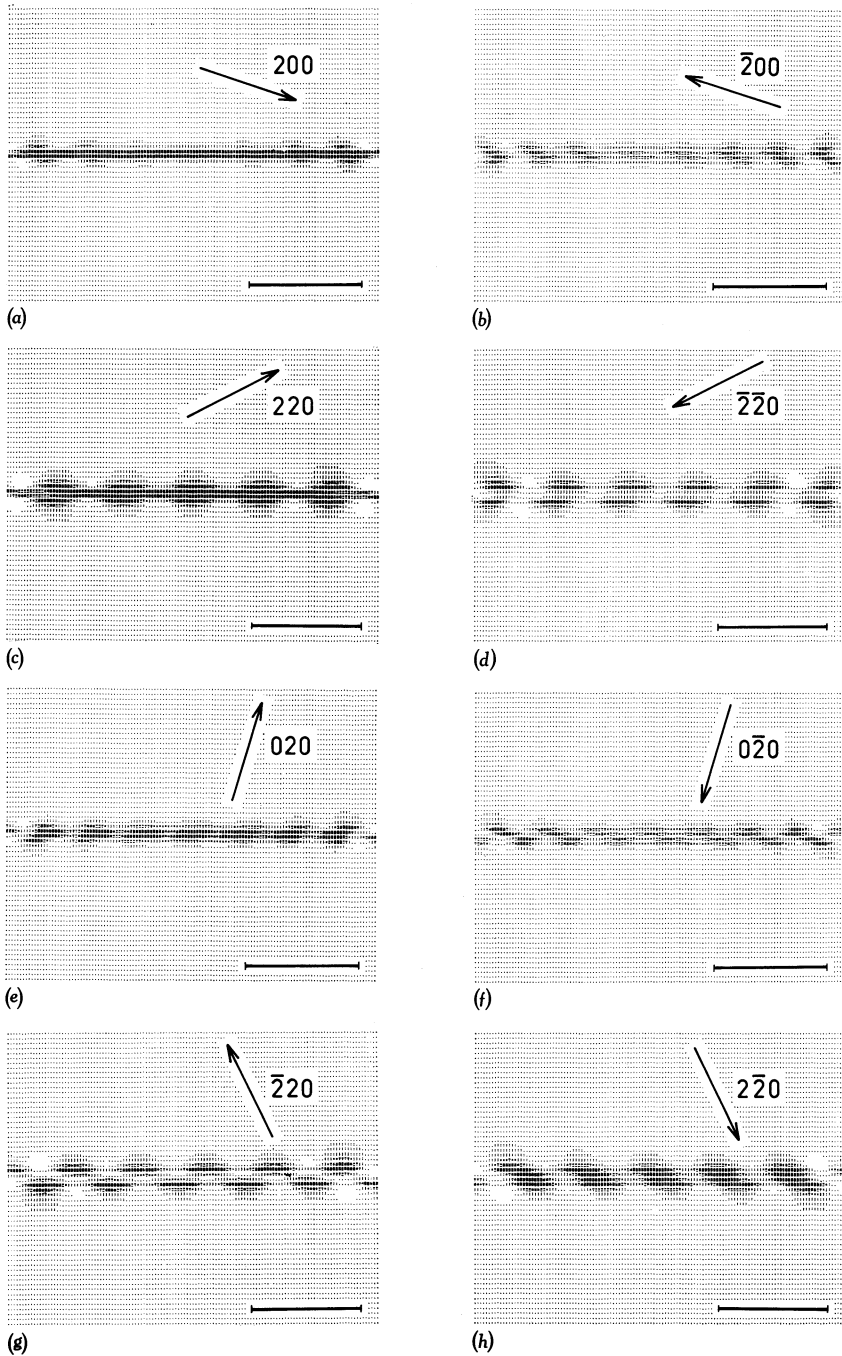
Fig. 1.—Theoretical images of a line of expansion for the eight low order face-centred cubic reflections contained in the [001] beam direction. The line lies along [314], the foil normal is [$\bar{1}$15], and the deviation from the Bragg condition, $w$, is 0·6. The length of the marker is 500 Å.
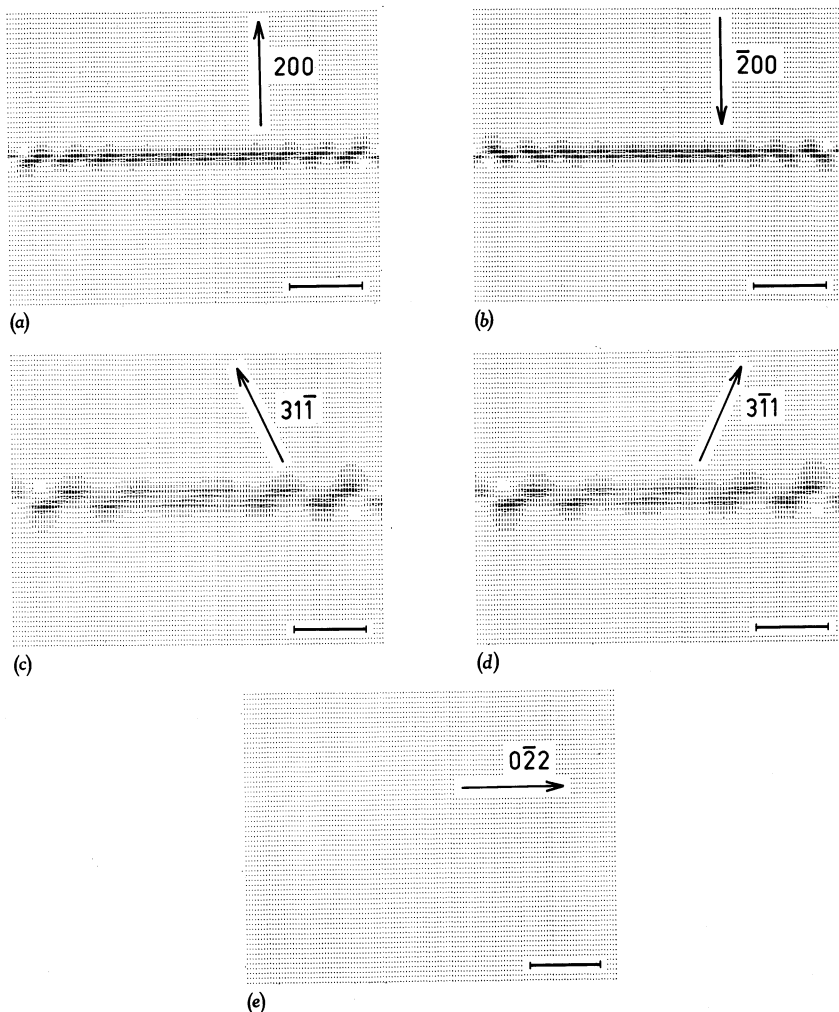
Fig. 2.—Theoretical images of a line of expansion illustrating the symmetry properties for $+\mathbf{\dot{g}}$ and $-\mathbf{\dot{g}}$, (a) and (b); for equally inclined diffracting vectors, (c) and (d); and the occurrence of the invisibility criterion, (e). The line lies along [0$\bar{1}$1], the beam direction is [011], the foil normal is [001], and the deviation from the Bragg condition, $w$, is $0\cdot6$. The length of the marker is 500 Å.

Fig. 3 (*opposite*).—Comparison of the image of a pure edge dislocation (a), representing the insertion of an extra half plane of atoms into the crystal, with the image of a line of expansion (b), representing the insertion of an extra row of atoms into the crystal. The line of the defects lies along [112], the beam direction is [001], the foil normal is [$\bar{1}$15], and the deviation from the Bragg condition, $w$, is $0\cdot6$. The length of the marker is 100 Å.

Fig. 4 (*opposite*).—Theoretical images of a line of contraction. In (a) and (b) the strength of the contraction is the same as that of the line of expansion shown in Figure 1, and in (c)–(f) the strength is only $0\cdot1$ of this. The visibility limits are 15% above and 7% below background intensity for (a)–(d) and 5% above and 2% below background intensity for (e) and (f). The diffraction conditions and geometry are the same as for Figure 1. The length of the marker is 500 Å.
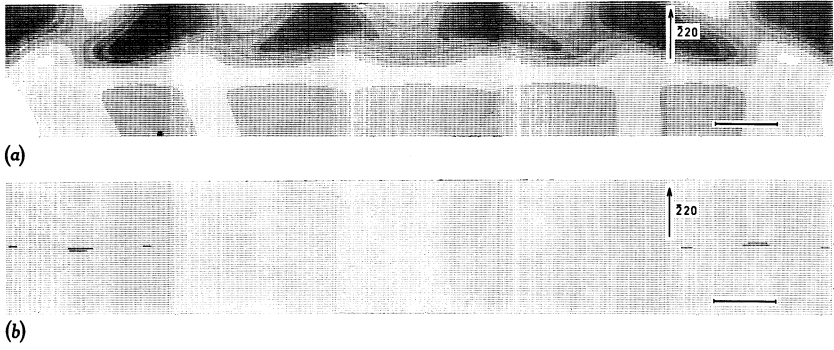
Fig. 3
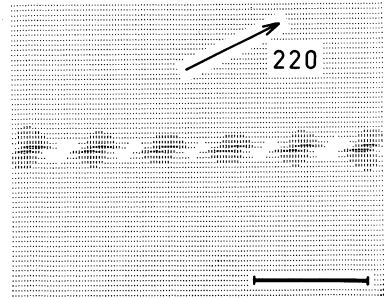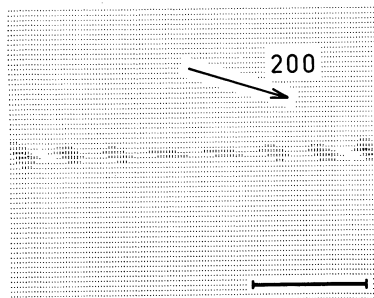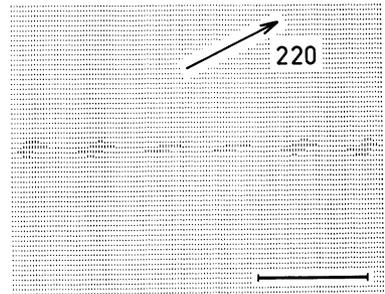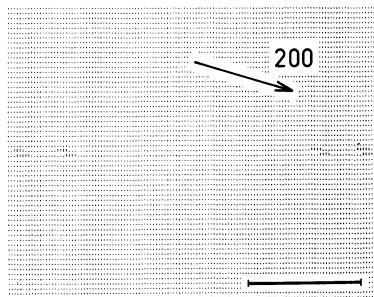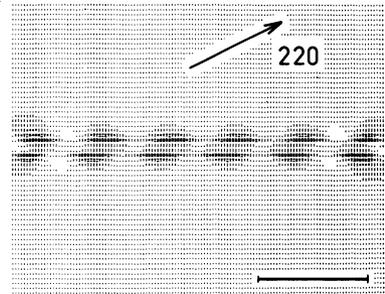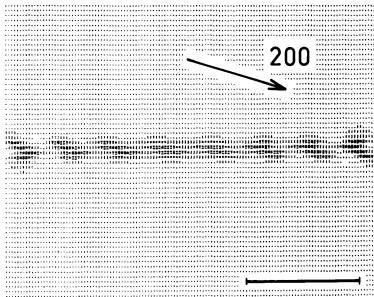


Fig. 4

of dilation, and the beam direction are all coplanar. On the other hand, it is not a necessary condition for this effect that the dilation line lies in a plane normal to the beam direction as it does in Figures 2(c) and 2(d).

The condition for invisibility of a line of dilation in centrosymmetric, elastically isotropic crystals is that the reflecting vector lies exactly along the dilation line. This can only occur, therefore, when the line lies in the plane normal to the beam direction. In Figure 2(e) the reflecting vector $0\bar{2}2$ lies along the same line of dilation depicted in the other micrographs in Figure 2, and it can be seen that there is no contrast whatsoever. This condition for invisibility is, of course, the same as that for pure edge dislocations in similar media.

The differential equations of Howie and Whelan describing the contrast from defective crystals (e.g. Howie and Whelan 1962, equations 5 and 6) involve the derivative of the displacement function of the particular defect. It can be seen from equation (1) that the derivative of the displacement due to a line of dilation varies as $1/r^2$; that due to a dislocation varies as $1/r$. It is to be expected, therefore, that for similar displacements at the cores* of these defects, the images of lines of dilation will be narrower than the images of dislocations. This is illustrated in Figure 3. The image shown in Figure 3(a) is that of a pure edge dislocation lying along [112] with Burgers vector $\frac{1}{2}[\bar{1}10]$ imaged with the $\bar{2}20$ reflecting vector. Figure 3(b) shows the corresponding image of a line of expansion for which $\epsilon$ is half an atomic diameter and $\Delta\epsilon = \epsilon$. Thus in these figures we are comparing the image of a defect that consists of an extra half plane of atoms inserted into the crystal (Fig. 3(a)) with that of a defect that is an extra row of atoms (Fig. 3(b)), and the displacements in the immediate neighbourhood of the cores of these defects are therefore similar. The differences in both the width and the overall intensity of the images in Figure 3 are obvious.

So far, we have considered only expansions rather than contractions. Two images for a line of contraction with $\epsilon = 3$ and $\Delta\epsilon = -\epsilon$ are shown in Figures 4(a) and 4(b) for the 200 and 220 reflecting vectors. The other conditions are the same as for the micrographs shown in Figure 1 and it should be noted that the images in Figures 4(a) and 4(b) are identical with those in Figures 1(b) and 1(d) respectively, i.e. with a line of expansion imaged under the negative reflecting vector.

One model for a line of contraction is to consider the relaxation of a line defect containing vacancies. However, because of the nature of the law of force between atoms, the displacements (due to relaxation) around such a defect are likely to be much smaller than those (due to compression) for the equivalent defect containing interstitial or impurity atoms. Thus, the value of $\Delta\epsilon$ for a line of contraction will be less than $|\epsilon|$. This, together with the narrowness of the images, indicates that images from lines of contraction encountered experimentally will probably be extremely faint. This tendency has been illustrated in Figures 4(c) and 4(d) for a line of contraction similar to that imaged in Figures 4(a) and 4(b), where $\epsilon = 3$ but $\Delta\epsilon$ is only $-\epsilon/10$.

---

* The term "core" is used here in connection with lines of dilation with the same meaning and for similar reasons to the way it is used in dislocation theory. In the case of the particular example quoted above, it is assumed, for the purpose of comparison, that the core of the dislocation and that of the dilation have similar dimensions.

## Discussion

From the properties described in the previous section, it can be seen that lines of dilation may best be identified by three main factors:

(1) the centre of inversion symmetry of their images,
(2) the unrelated nature of images on $+\mathbf{g}$ and $-\mathbf{g}$, and
(3) the invisibility of the image with a reflecting vector along the line.

Either of the factors (1) or (2) is sufficient to distinguish the images of a line of dilation from that of a single dislocation under normal conditions. However, it should be pointed out that images of multiple dislocation configurations can have different symmetry properties from those of a single dislocation. Indeed, it has been found (Humble, unpublished work) that two closely spaced glide dislocations of opposite sign (i.e. a dipole) can have images with very similar symmetry properties and character to those of a line of dilation. Since the image of a line of expansion taken on $+\mathbf{g}$ is exactly the same as that of the corresponding line of contraction taken on $-\mathbf{g}$ (compare Figs. 1(b) and 4(a), and Figs. 1(d) and 4(d)), then, if the absolute sense of $\mathbf{g}$ is known, the factor (2) may be used to distinguish between these defects.

In order to illustrate clearly the various properties of the image, most of the micrographs shown here (Figs. 1, 2, 4(a), and 4(b)) have been computed for lines of dilation that have relatively large displacement fields. They have all been printed using a grey scale that has effective visibility limits of 15% above and 7% below background intensity. However, it has been shown (Humble 1968b) that when viewing faint objects, the visibility criteria may drop as low as 5% above and 2% below background intensity. Thus it is to be expected that even the micrographs of weak lines of dilation (Figs. 3(b), 4(c), and 4(d)) may be readily detected experimentally and their symmetry properties recognized. For example, Figures 4(c) and 4(d) have been recomputed and printed in Figures 4(e) and 4(f) using a grey scale that has visibility limits 5% above and 2% below background intensity. It may be seen that the characteristics of these images are now clearly demonstrated.

There are several instances where defects of the sort considered here are likely to occur. The most obvious case is that of irradiated crystals. Blank and Amelinckx have investigated fission tracks in uranium dioxide crystals and have attributed some of the contrast effects observed in thin foils of these examined in the electron microscope to the presence of lines of dilation. However, the contrast from these tracks is extremely weak (they are thought to be lines of contraction rather than expansion; Amelinckx, personal communication) and the general symmetry properties are not apparent in their micrographs. Only the condition for invisibility enabled the tracks to be identified as lines of contraction or dilation.

Other cases where these defects are likely to occur are in crystals quenched from high temperature, when vacancies or gas dissolved in the lattice may precipitate out along preferred directions. Retchford (personal communication) is investigating the possibility that some of the defects observed in synthetic quartz may be due to the precipitation of water vapour along preferred directions in the crystal lattice. In general, vacancies in quenched metals tend to precipitate as planar or three-dimensional defects, and, to the author's knowledge, no lines of contraction have been observed experimentally in such materials.

P. HUMBLE

    The condensation of vacancies on dislocation lines usually jogs the dislocations
so that they climb out of their slip plane.  However, it is possible that the vacancies
could form a quenched-in atmosphere around the dislocations, and, of course, the
existence of atmospheres of impurity atoms around dislocations especially in body-
centred cubic metals (e.g. carbon or nitrogen in iron) is well established (e.g. Cottrell
1961).  Several images of a combined dislocation line and line of dilation have been
computed, but these are so complex that no useful general properties can be deduced.
Where such configurations are suspected, each image will have to be computed for the
particular conditions of observation.

## REFERENCES

ASHBY, M. F., and BROWN, L. M. (1963).—*Phil. Mag.* **8**, 1083.
BLANK, H., and AMELINCKX, S. (1963).—*J. appl. Phys.* **34**, 2200.
COKER, E. G., and FILON, L. N. G. (1957).—"Photoelasticity." p. 299. (Cambridge Univ. Press.)
COTTRELL, A. H. (1961).—"Dislocations and Plastic Flow in Crystals." (Oxford Univ. Press.)
HEAD, A. K. (1967).—*Aust. J. Phys.* **20**, 557.
HEAD, A. K. (1969).—*Aust. J. Phys.* **22**, 43.
HEAD, A. K., Loretto, M. H., and Humble, P. (1967).—*Phys. Status Solidi* **20**, 505.
HIRSCH, P. B., HOWIE, A., NICHOLSON, R. B., PASHLEY, D. W., and WHELAN, M. J. (1965).—
    "Electron Microscopy of Thin Crystals." p. 496. (Butterworths: London.)
HOWIE, A., and WHELAN, M. J. (1961).—*Proc. R. Soc.* A **263**, 217.
HOWIE, A., and WHELAN, M. J. (1962).—*Proc. R. Soc.* A **267**, 206.
HUMBLE, P. (1968a).—*Aust. J. Phys.* **21**, 325.
HUMBLE, P. (1968b)—*Phys. Status Solidi* **30**, 183.